https://doi.org/10.5194/hess-2024-351
Preprint. Discussion started: 3 February 2025

Hydrology and Earth System Sciences Discussions

Evaluation of remote sensing algorithms for estimating actual evapotranspiration in arid agricultural environments

Phathutshedzo Eugene Ratshiedana [1, 2] Mohamed A. M. Abd Elbasit 3, Elhadi Adam[1] and Johannes George Chirima [2, 4]

[1]School of Geography, Archaeology and Environmental Studies, University of the Witwatersrand, Johannesburg Private Bag x3, Wits, Johannesburg 2050, South Africa
[2]Agricultural Research Council−Natural Resources and Engineering−South Africa, 600 Belvedere Street, Arcadia, Pretoria 0083, South Africa
[3]Department of Physical and Earth Sciences, School of Natural and Applied Sciences, Sol Plaatje University, Kimberley 8300, South Africa
[4]Department of Geography, Geoinformatics and Meteorology, University of Pretoria, Pretoria 0028, South Africa

Correspondence to: Phathutshedzo Eugene Ratshiedana (Ratshiedanap@arc.agric.za)

Abstract. Accurate estimation of actual evapotranspiration (ETa) at both field and larger spatial scales is crucial for understanding crop water use and hydrological interactions particularly in arid regions facing water scarcity. In South Africa, ETa data gaps hinder effective agricultural water management. Advances in geospatial techniques combining Geographical Information Systems (GIS) and remote sensing have made it possible to estimate ETa over large areas. However, the reliability of this depends on the accuracy of algorithms used which must be validated against ground measurements. With the lack of direct ETa measurements in South Africa, this has been a challenging task. This study evaluated ETa variability at farm level to the level of an irrigation Scheme, covering over 36,000 hectares. A total of 22 Landsat 8 satellite images from 2019 to 2021 were used to estimate ETa based on four algorithms: the Surface Energy Balance Algorithm for Land (SEBAL), Surface Energy Balance System (SEBS), Vegetation Index (VI)-based ETa and Crop Water Stress Index (CWSI)-based ETa. Field-scale estimates were compared to measurements from a smart field weighing lysimeter, while larger-scale estimates were validated against extrapolated ETa values. The SEBAL, SEBS and VI-based ETa algorithms correlated well with field-scale lysimeter data, while the CWSI-based algorithm showed poor correlation. SEBAL emerged as the best-performing algorithm, with high correlation coefficients (r=0.91-0.96), strong R^2 values (0.83-0.92) and the lowest errors (RMSE 0.31-0.89 mm d^{-1}, MAE 0.27-0.82 mm d^{-1}). Findings from this study forms a foundation of improved water management strategies to reduce the overuse of water in agriculture.

1 Introduction

Evapotranspiration (ET) is a critical component in hydrological studies representing a bi-directional process encompassing both evaporation of soil water content, water from other land cover surfaces and losses though transpiration from vegetation canopy (Pandey et al., 2016; Raza et al., 2022). In agricultural settings, actual evapotranspiration (ETa) serves as a crucial

https://doi.org/10.5194/hess-2024-351
Preprint. Discussion started: 3 February 2025


Hydrology and Earth System Sciences Discussions

measure for quantifying crop water use (Djaman et al., 2023). Accurate quantification of ETa allows farmers to determine precise crop water requirements as water lost through the process of ET which must to be replenished through irrigation (Elfarkh et al., 2022; Djaman et al., 2023). In irrigation schedules where ETa is not quantified, the likelihood is that farmers will either over-irrigate or under−irrigate. The overuse of water in irrigation contributes largely to the continuous depletion of the available scarce water resources. In alternate scenarios, crops might suffer water logging conditions and salinity problems, which can impact crop yields negatively (Ingrao et al., 2023).

Monitoring and managing agricultural water resources requires accurate measurement of ETa, however, this requires expensive devices which are not practical to deploy across larger extents (Sharma et al., 2015; Djaman et al., 2019). For many decades, crop evapotranspiration (ETc) has been estimated using meteorological methods requiring data acquired from weather stations (Meyer, 1926). These stations are still not enough in most parts of South African agricultural landscapes (Ncoyini et al., 2022). The Food and Agriculture Organization (FAO) has provided crop coefficient (Kc) values for a wide range of crops cultivated globally to aid in estimating ETc (Allen et al., 1998). However, the original Kc values were developed outside South Africa and were not specifically tailored for horticultural or non-agricultural vegetation while in agriculture they were not developed using drought−resistant cultivars which of lately are prevalent in the country's arid regions (Mulovhedzi et al., 2020; Mukiibi et al., 2023). According to Allen et al. (1998) ETc can be estimated by multiplying the crop specific Kc values by the reference evapotranspiration (ETo) value. The Kc values are determined as the ratio of ETa to ETo, with ETo calculated using meteorological variables with models like the Penman-Monteith and Dalton amongst others (Dalton, 1802; Allen et al., 1998). However, ETa on the ground is typically derived using specialized equipment such as lysimeters, although these devices offer high accuracy representation of actual water use, they are point instruments which are limited in their ability to represent the spatial variability of ETa particularly in heterogeneous landscapes (Doležal et al., 2018; McNamara et al., 2021).

With ETa being key in development of Kc values and determining the true reflection of crop water consumption, South Africa faces a substantial gap in the direct measurement of ETa primarily due to the limited availability of the necessary devices for this purpose. This limitation is highlighted in the study of (Meijninger and Jarmain, 2014), who could not validate satellite ET estimates from a remote sensing-based model in Kwazulu-Natal. The country has only two FLUXNET eddy covariance stations providing open-access data, with other stations being privately owned and inaccessible for national water management efforts (Blatchford et al., 2020).

With the economic impracticality of quantifying water use for the vast diversity of vegetation species worldwide and the logistical challenges of conducting ground experiments for millions of species, remote sensing can provide estimates of ET over large areas, providing an alternative to ground-based measurements which often lack the spatial coverage and sometimes the temporal resolution required for effective water management (Tan et al., 2021; Saha et al., 2022; Tran et al., 2023). However, the success of remote sensing in ET estimation depends on the availability of high accuracy measuring devices and

https://doi.org/10.5194/hess-2024-351
Preprint. Discussion started: 3 February 2025


Hydrology and Earth System Sciences
Discussions

good algorithms capable of calibrating remotely sensed images for precise ET determination (Li et al., 2023; Tran et al., 2023). Satellite-derived ET estimates can be influenced by factors such as cloud cover, atmospheric conditions, sensor saturations and their spatio-temporal resolution (Mckenzie et al., 1998; Wang et al., 2023). In regions with heterogeneous landscapes and variable cropping patterns, these challenges are further exacerbated leading to discrepancies between satellite-derived ET estimates and ETa observed in the field (Lian et al., 2022).

Several ET algorithms have been developed, applied and validated across different environments (Zamani and Rahimzadegan, 2018). These algorithms include the Surface Energy Balance Algorithm for Land (SEBAL), Mapping Evapotranspiration at High Resolution with Internalized Calibration (METRIC), Atmosphere Land Exchange Inverse (ET-ALEXI), Surface Energy Balance (SEBS) and the Three-Temperature Model (3T Model) amongst others (Bastiaanssen, 2000; Allen et al., 2007; Yan, 2016). Studies involving the utilization of remote sensing data for assessing water use and hydrology in South Africa have been conducted employing the SEBAL algorithm alongside data from Landsat at different scales (Shoko et al., 2015; Ndou et al., 2018; Singels et al., 2018). These studies reported the lack of accurate measured ET which was measured using devices with known inaccuracies such as eddy covariance systems. However, Bastiaanssen et al. (2005) reported that the SEBAL algorithm can have an accuracy of about 85% at field scale while it can be improved to over 95% if applied across different seasons. However, studies focusing on SEBAL seasonality impact are still lacking in South Africa. Gibson et al. (2013) suggested that future research using the SEBS algorithm in South Africa should focus exclusively on agricultural landscapes. This recommendation arises from the limitations of ET algorithms when applied to a wide range of land use types.

Vegetation index-based evapotranspiration (VI-ETa) approaches have been proven to be effective in estimating ETa across diverse regions. For instance, Glenn et al. (2010) reviewed the combination of ground-based ETa measurements with VI-ETa methods across different biomes obtaining strong correlations with coefficients of determination ranging between 0.45 and 0.95. Their findings indicate correlations between 0.67 and 0.97, with which they suggested that VI-ETa algorithms can be more accurate when calibrated with accurate ground measurements such as those obtained from weighing lysimeters. Jiang et al. (2020) emphasized that errors in ETa estimates can be reduced to within 5% using such devices, while Hunsaker et al. (2005) demonstrated similar precision. Nagler et al. (2013) used MODIS EVI to estimate ETa in riparian and agricultural areas achieving less than 10% error when compared to eddy covariance measurements. They recommended VI-ETa models for drylands where non-vegetative factors are minimal and suggested the Penman-Monteith or Blaney-Criddle methods for areas lacking ETa data. Abbasi et al. (2021) applied VI-ETa using Landsat imagery to monitor agricultural drought in Iran, despite the lack of ground data in the country. They found that VI-ETa estimates correlated well with in-situ data at the basin scale, with errors ranging from 15 to 21%, and from 2.5 to 34% at the country scale. These studies highlight the potential of VI-ETa to accurately estimate crop water use provided accurate calibration data such as data from weighing lysimeters is available. In South Africa, VI-ETa use remains limited due to challenges in obtaining precise ETa measurements for calibration. Furthermore, the use of crop water stress index (CWSI) for determining ETa remains unexplored in the country.

https://doi.org/10.5194/hess-2024-351
Preprint. Discussion started: 3 February 2025


Hydrology and Earth System Sciences Discussions

The Vaalharts Irrigation Scheme which is one of the largest in South Africa requires accurate ETa estimation for optimizing water usage and ensuring sustainable agricultural practices. This is because the scheme sources water from areas such as the Vaal River through the Bloemhof dam with ample water to sustain irrigation (Maisela, 2007). Water in the scheme is only monitored from discharge points for billing purposes using flow meters, however, the amount of water used by crops and the surrounding vegetation after each irrigation event remains unknown. Given the limitations of ETa variability data, there is a pressing need for research focused on evaluating and improving the accuracy of ETa algorithms.

This study aims at evaluating the capabilities and accuracies of SEBAL, SEBS, VI-based ETa and the CWSI-based ETa algorithms using an integration of a high precision smart field weighing lysimeter and automatic weather stations approach. The specific objectives were: (i) to use ETa measurements by a smart field weighing lysimeter across four cropping seasons to validate estimates from the four algorithms at field scale and, (ii) to extrapolate ETa from lysimetric measurements to other locations with weather stations. This is the first study to evaluate remotely sensed ETa using a smart field weighing lysimeter as demonstrated by (Tran et al., 2023) that lysimeter approach in South Africa is uncommon on their review study. This study contributes to the broader field of remote sensing offering more information on the strengths and limitations of these algorithms in diverse agricultural landscapes to solve the irrigation water management and ETa data scarcity challenges.

2 Methods and materials

2.1 Study area description

This study was conducted within the Vaalharts irrigation scheme located in the Northern Cape province of South Africa between the coordinates: 24°44'16.91"E and 27°38'33.23"S on the North, while on the Southern parts the scheme starts at 24°37'37.46"E and 28° 4'54.38"S. The irrigation scheme is the largest irrigation scheme in South Africa covering over 36 950 hectares (Ojo et al., 2011). The scheme is located between two plateaus, and its terrain is low-lying, with elevations ranging between 1080 and 1 137 m above sea level (asl). The scheme receives irrigation water through a canal system with water coming from the Bloemhof dam, the dam which is fed by the Vaal River. Additional water comes from the Harts River were water goes into the irrigation scheme facilitated by a diversion weir located in Warrenton town, the weir collects water from the Harts and Bloemhof dam into the scheme. The study area experiences low annual rainfall averaging between 400 and 500 mm $year^{-1}$ (Moeletsi et al., 2022). Several crops are planted including maize, wheat, barley, cotton, soybeans, groundnuts, watermelon and various fruit trees such as pecans and olives (Pretorius, 2018; Ratshiedana, 2022). The soils within the scheme are alluvial soils prone to salinization (Ojo, 2013). Pivot irrigation systems dominate the area, while other forms of irrigation, such as flood irrigation, bubblers, sprinklers and drips, are common (Maisela, 2007; Verwey and Vermeulen, 2011; Ratshiedana, 2022). The irrigation scheme supports both small-scale and large-scale farming operations. The importance of

https://doi.org/10.5194/hess-2024-351
Preprint. Discussion started: 3 February 2025

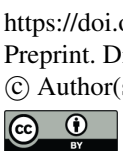

Hydrology and Earth System Sciences
Discussions

this scheme lies in it being a major source of employment and food security and contributing significantly to the local economy where most agricultural enterprises emerged to support farming and retail was developed to support the farming communities residing around the scheme (Maisela, 2007). The study area comprises of an 18-ha experimental farm and four validation sites with automatic weather stations with station locations named: SABBI, Tadcaster, Jankempdorp and Ganspan (Fig.1).

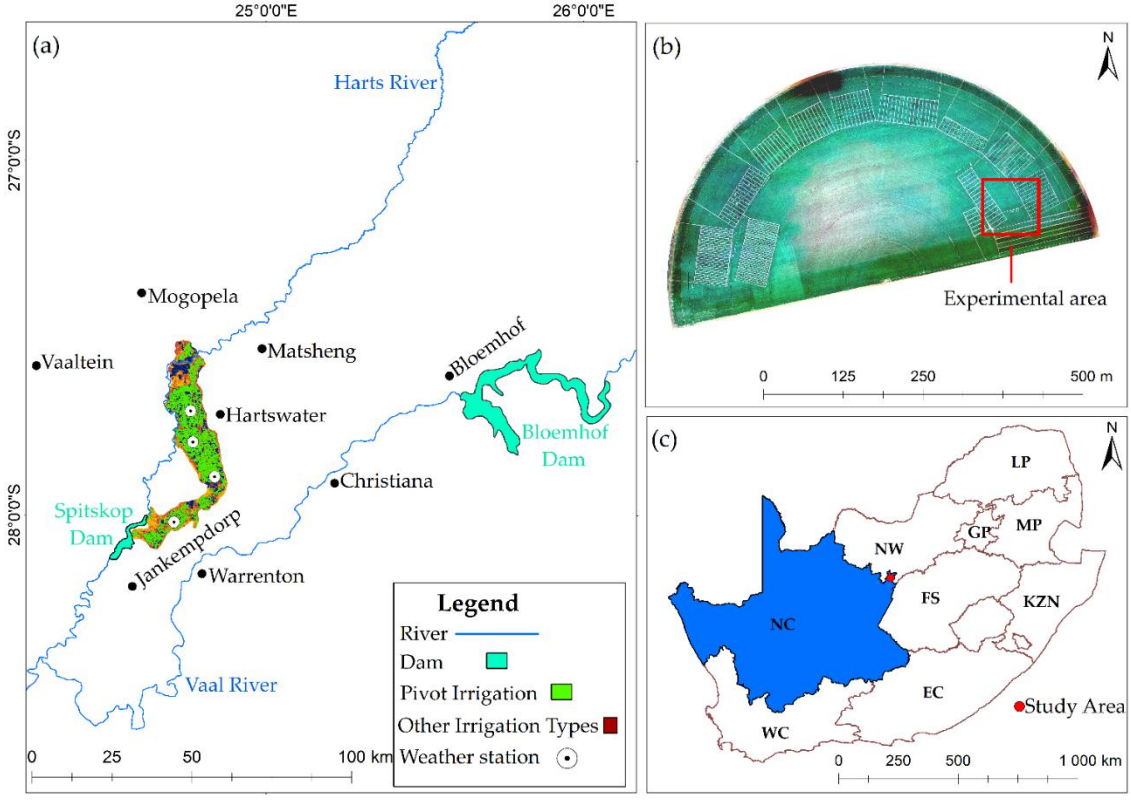

Figure 1. Map showing the study area distinct regions, (a) delineates the Vaalharts irrigation scheme, its surrounding towns, major rivers and dams, (b) shows the (18-ha) experimental farm, and (c) indicates the study area's position in relation to various provinces.

2.2 Research approach

Having identified that direct measurement of ETa in South Africa is the limiting factor in evaluating remote sensing ETa products and algorithms. This study focuses on the use of a smart field weighing lysimeter as an accurate tool for measuring ETa to enable the evaluation and calibration of four ETa algorithms. Ground-based measurement and monitoring techniques were used for validation, while satellite-based monitoring provided a continuous and cost-effective source of information. These measurements developed a large-scale validation proxy using meteorological information considering the scarcity of data in an agricultural landscape. The research approach is summarised in the conceptual representation below (Fig.2).

https://doi.org/10.5194/hess-2024-351
Preprint. Discussion started: 3 February 2025

Hydrology and Earth System Sciences
Discussions

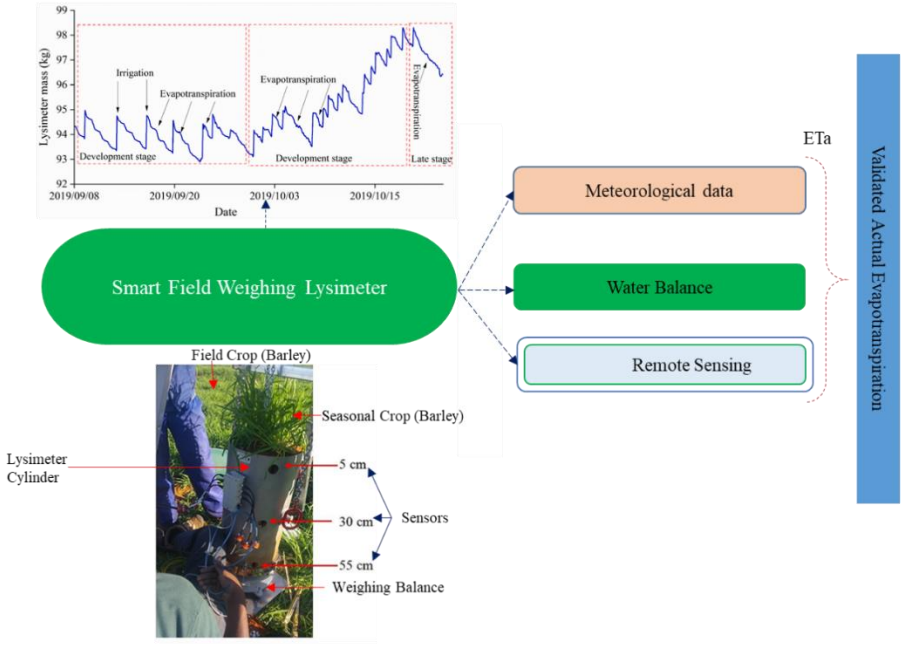

Figure 2. Conceptual framework for the study approach linking satellite data and ground measurements.

2.3 Data Acquisition

2.3.1 Satellite data acquisition and pre-processing

Remotely sensed Landsat 8 images with multiple bands were obtained from the United States Geological Survey (USGS) Earth Explorer portal (https://earthexplorer.usgs.gov/ Accessed: 04 February 2023) using a bulk downloader for automatic and continuous download of the specified data (Table 1). A total of 22 images were acquired for the study period, their cloud cover % are given in Table (S1). The Level 1 Terrain Corrected (L1T) were retrieved covering a period between 1st September 2019 and 31 May 2021. The pre-processing of Level 1 Terrain Corrected (L1TP) data was executed using the Semi-Automatic Classification Plugin (SCP) in QGIS. Radiometric calibration was done to transform digital numbers (DN) to top-of-atmosphere (TOA) reflectance. This conversion was achieved by utilizing the metadata linked to each image file. Since the L1TP data had already been georeferenced, geometric correction was unnecessary. Atmospheric correction was applied to mitigate the impact of atmospheric scattering and absorption. For the thermal bands, processing was carried out to derive temperature values in degrees Celsius (°C) while they were also resampled to 30 m to match the multispectral bands.

https://doi.org/10.5194/hess-2024-351
Preprint. Discussion started: 3 February 2025

Hydrology and Earth System Sciences Discussions

Table 1. Landsat 8 Satellite Data used for estimating ETa

Band Name	Wavelength
Band 2 - Blue	0.45-0.51 nm
Band 3 - Green	0.53-0.59 nm
Band 4 - Red	0.64-0.67 nm
Band 5 - Near Infrared (NIR)	0.85-0.88 nm
Band 6 - Short-wave Infrared (SWIR) 1	1.57-1.65 nm
Band 7 - Short-wave Infrared (SWIR) 2	2.11-2.29 nm
Band 10 - TIRS 1	10.60-11.19 µm
Band 11 - TIRS 2	11.50-12.51 µm

2.3.2 Smart field weighing lysimeter measurement and evapotranspiration calculation

A smart field weighing lysimeter by METER Group© was used to measure field soil-water-crop interactions. The lysimeter used is cylindrical in shape with 60 cm height and a diameter of 30 cm with the surface area of 0.07 m^2. This lysimeter contains a suite of sensors which measure soil water content fluxes, soil temperature, matric potential, soil electrical conductivity and contains weighing balances that measure the lysimeter mass and another balance measuring the drainage amount outside the lysimeter cylinder. The weight losses are related to soil water evaporation and crop transpiration, while mass gains are related to irrigation or precipitation events. The lysimeter used offers real-time monitoring and high temporal resolution data at an interval of 1 minute on mass balances, while sensors measurements were done at 10 minutes interval. The process of calculating ETa from smart field weighing lysimeter data was done using R in Posit Software (PBC), formerly known as RStudio (https://posit.co/). The processing was focused on aggregating hourly measurements to daily totals to match with the daily ETa estimated by the satellite images. The *tidyverse* and *lubridate* packages were used to prepare the data by extracting the date component from the timestamp. The daily ETa values were visualized using the *ggplot2* package to identify patterns or anomalies and the results were exported as .csv for further analysis. The exported data was further processed using the Savitzky-Golay filtering technique on Originlab© software to smooth ETa data were un-explainable spikes existed as done by Peters et al. (2014). Evapotranspiration was computed using the changes in lysimeter and drainage balances weight with irrigation negligible during zero-irrigation days using Eq. (1):

$$ETa = I - \Delta D - \Delta S \quad (1)$$

where ETa I is irrigation or precipitation in mm, ΔD is the change in the drainage mass balance in kg whereas, ΔS is the change in lysimeter mass balance (kg).

https://doi.org/10.5194/hess-2024-351
Preprint. Discussion started: 3 February 2025


Hydrology and Earth System Sciences Discussions

Based on the measured parameters, the above formula can be represented using the simplified Eq. (2):

$$ETa = (Lm(n) + Dm(n) - Lm(n-1) + Dm(n-1) \times 14.14 \quad (2)$$

where Lm (n) is the lysimeter mass in kg at time "n", Dm (n) is the drainage mass in kg at tine "n", Lm (n−1) is the lysimeter mass at time "n−1", while Dm (n−1) is the drainage mass in kg at time "n−1". The value 14.14 was obtained based on the assumption that, 1 kg of water seepage in the lysimeter equals 0.001 m^3 which when divided by the surface area of the lysimeter it gives 0.014 m which is equivalent to 14 mm, as a result each 1 kg equalled 14 mm.

2.3.3 Meteorological data

An ONSET HOBO remote monitoring system (RX3000) automatic weather station was used to measure all meteorological variables at field level. The operating range of the station is -40 to 60 °C while it does support remote communications with its continuous solar power supply supporting the battery life. The station was configured with different soil sensors including moisture and temperature sensors while it provided cloud-based data access through HOBOlink. The stations used for the purpose of calibration and validation of remotely sensed variables were the automatic weather stations owned by the Agricultural Research Council (ARC) of South Africa. The stations are equipped with humidity sensors, air temperature, wind speed sensors, wind direction, gust sensor, rain gauge, barometric sensors, soil moisture sensors and solar radiation sensors (Moeletsi et al., 2022). Each weather station is installed at a height of 1.2 m. The meteorological information is retrieved remotely and can be accessed through: https://www.arc.agric.za/arc−iscw/Pages/Agrometeorology−Reports.aspx accessed on 16 June 2023. For this study, the data required was extracted for the times September 2019 to end of May 2021.

2.4 Remote sensing-based evapotranspiration algorithms

2.4.1 Vegetation Index-Based Evapotranspiration (VI-ETa) estimation

The VI-ET algorithm is a remote sensing technique which is used to estimate ETa by incorporating vegetation indices (VIs) such as the Normalized Difference Vegetation Index (NDVI) or Enhanced Vegetation Index (EVI) (Glenn et al., 2010). These indices are derived from any multispectral satellite imagery which can reflect vegetation health, canopy density and their state of greenness. The algorithm integrates these indices with ETo derived from meteorological data for the purpose of determining Kc values at different vegetation growth stages representing the relationship between vegetation status and water use (Nagler et al., 2013). The VI-ETa algorithm then estimates ETa by multiplying the VI-based Kc by meteorological derived ETo to enable the modelling of spatially distributed estimates of vegetation water use across different land covers. This algorithm was selected based on its ability to provide detailed spatial resolution over large areas, making it suitable for field scale, regional or even global ETa estimation. The general equation for ETa or ETc which resemble the same component is given by Eq. (3):

https://doi.org/10.5194/hess-2024-351
Preprint. Discussion started: 3 February 2025


Hydrology and Earth System Sciences
Discussions

$$ETa = ET_o \times Kc \quad (3)$$

The values of Kc were derived at field scale using the FAO procedure (Allen et al., 1998) as the ratio of ETa to ETo using Eq. (4):

$$Kc = \frac{ETa}{ETo} \quad (4)$$

The ETo which incorporates the variability in weather conditions was determined using R from an automatic weather station data using the standard Penman-Monteith equation introduced by Allen et al. (1998) given as Eq. (5):

$$ET_o = \frac{0.408\Delta(R_n - G) + \gamma\left(\frac{C_n}{T+273}\right)U_2(e_s - e_a)}{(\Delta + \gamma(1 + C_d U_2))} \quad (5)$$

where the symbol Δ is the slope of saturation vapour pressure (kPa °C^{-1}). The term Rn corresponds to the total radiation on the vegetation surface (MJ m² d^{-1}) over a 24−hour period, while the term G denotes the heat flux density. The average daily air temperature is indicated as T (°C), while the term U_2 is the average hourly wind speed measured at a height of 2 m (m s^{-1}). The variable es denotes the saturation vapour pressure (kPa), while e_a signifies the actual vapour pressure (kPa). The difference of $e_s - e_a$ indicates the saturation vapour pressure deficit (kPa). The term γ is the psychrometric constant (kPa °C^{-1}), whereas Cn and Cd are constants that vary based on the reference crop surface being used (Allen et al., 1998).

The Kc values were determined for every satellite pass date based on the measured ETa and the determined ETo at farm level. The measurement of ETa was only based on one farm within the entire irrigation scheme due to limitation of ETa measuring device in the scheme. As a result, the relationship between Kc values and NDVI was used to model the Kc for the entire irrigation scheme using the approach used by Niu et al. (2020) for estimating Kc spatial variability. The determination of Kc was done for four cropping seasons at the farm level resulting in four Kc models which were amalgamated into an ensemble Kc model. The determination of Kc was done on QGIS using the NDVI layer using Eq. (6):

$$Kc = a \times DNVI + b \quad (6)$$

where a and b are the coefficients from the relationship between NDVI and Kc

https://doi.org/10.5194/hess-2024-351
Preprint. Discussion started: 3 February 2025

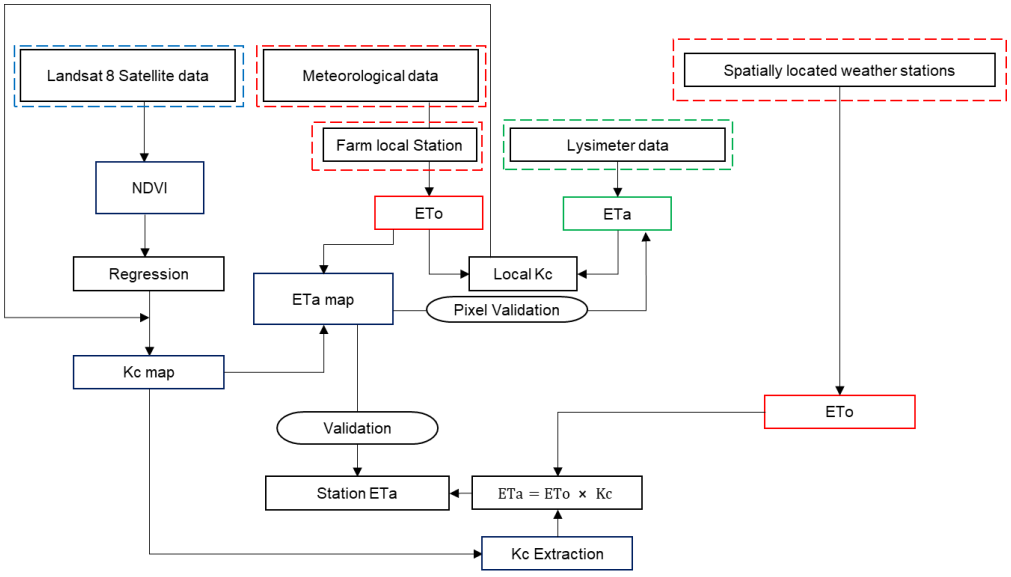

250 **Figure 3. The workflow for VI-ETa algorithm's actual evapotranspiration estimation and validation. The workflow integrates various steps including data processing, generation of the ETa maps and accuracy validation steps.**

2.4.2 The SEBAL Model

The Surface Energy Balance Algorithm for Land (SEBAL) is a remote sensing algorithm used to estimate ETa based on thermal and multispectral datasets across large areas by calculating the energy balance of the Earth's surface. This algorithm
255 was developed by Bastiaanssen in the early 2000s with the purpose of using images to analyse the exchange of energy between the land surface and the atmosphere above it to the rate of water losses through evaporation and transpiration (Bastiaanssen, 2000). The retrieval of ETa was based on the energy balance approach using the SEBAL incorporated on the Surface Energy Balance and Crop Water Stress Spatial Analysis (SEBCS) plugin on QGIS which is given by Eq. (7):

$$\mathrm{ETa} = \mathrm{Rn} - \mathrm{G} - \mathrm{H} \tag{7}$$

260 where Rn represent the net radiation, G is the soil heat flux while H is the sensible heat flux and ETa is the evapotranspiration component equivalent to the latent heat flux (LE), all variables are measured in MJ m^{-2} d^{-1}.

2.4.3 Crop water stress-based ETa

Jackson et al. (1981) established a mathematical relationship between the crop water stress index (CWSI) and the vegetation water consumption. To compute ETa, they devised an approach given as Eq. (8):

265 $$\mathrm{ETa} = \mathrm{ETo} \times (1 - \mathrm{CWSI}) \tag{8}$$

https://doi.org/10.5194/hess-2024-351
Preprint. Discussion started: 3 February 2025


Hydrology and Earth System Sciences Discussions

The same formula was applied in this study using the Landsat 8 thermal data. The CWSI was calculated using the CWSI plugin on QGIS using thermal images, the outputs were multiplied by the sunshine hours for daily CWSI. The CWSI was computed based on Eq. (9):

$$\mathrm{CWSI} = \frac{\Delta T - \Delta Tm}{\Delta Tx - \Delta Tm} \quad (9)$$

where ΔT represents the difference in air temperature as determined by LST, ΔTm indicates the least change in LST_air, and ΔTx denotes the greatest divergence between LST and air temperature.

2.3.4 The Surface Energy Balance SEBS model approach

System (SEBS) was introduced by Su (2002) for estimating heat flow fluxes and evaporative fractions. This model shares similarities with the SEBAL model, with a distinction being the incorporation of soil heat flux in the SEBS model. The soil heat flux was calculated using Eq. (10):

$$G_o = R_n[T_c + (1 - F_{vc})(T_s - T_c)] \quad (10)$$

where Go is the soil heat flux, the term Rn represents the net radiation while Tc stands for the psychrometric constant for the canopy air layer. The variable Ts represents the psychrometric constant for the soil and Fvc is the fractional vegetation cover.

2.4 The validation of ETa algorithms at farm scale

2.4.1 Selection of validation pixels at field and irrigation scheme levels

One pixel was selected were the lysimeter and weather station were located at the experimental farm, the pixel represented estimate values at farm level from each algorithm. The validation of ETa derived the four algorithms evaluated was done by directly matching the ETa value measured from the smart field weighing lysimeter daily value with the ETa value estimated by the used algorithms across the 22 days in different cropping seasons at field scale. In the study area, only one farm was equipped with the smart field weighing lysimeter. The system could only validate ETa estimated at its location pixel for the four algorithms. However, to validate the effectiveness of the algorithms at different locations within the irrigation scheme, a relationship between Kc developed and ETo was used to estimate ETa using weather station locations. Direct comparisons between estimated ETa and extrapolated ETa were used for the validation process. However, the selection of validation dates were based on the periods when the scheme was entirely green during summer seasons when the area was not under intense water stress. This was to ensure that ETa is evaluated based on an active vegetation pixel than baresoil pixels, which would result in soil water evaporation possibly giving no values in such a water deficit environment. The spatial assessment was conducted for the models that demonstrated good results at the farm level with the assumption that poor-perfoming algorithms will likely not yield good results when transferred to different environments.

https://doi.org/10.5194/hess-2024-351
Preprint. Discussion started: 3 February 2025


Hydrology and Earth System Sciences Discussions

295 **2.4.2 Evaluation metrics**

The statistical metrics used for the evaluation process included the correlation coefficient (r), coefficient of determination (R^2), Root Mean Square Error (SE), Mean Absolute Error (MAE), Standard Error (SE) and Bias . The error metrics were used to determine the level of errors attributed to the used algorithms on their estimation of ETa compared to the measurements of ETa by the lysimeter. These metrics were selected because each of them captures a unique aspect of model accuracy and 300 reliability. The r and R^2 assess the strength and consistency of the relationship between estimated and measured values, highlighting the model's ability to explain variability. The RMSE and MAE quantify the magnitude of errors, with RMSE emphasizing large deviations and MAE providing an average error magnitude. The SE and bias evaluate the presence of systematic over- or underestimation, offering insights into the directional tendencies of the algorithms. In combination, these metrics ensure a strong evaluation by portraying both precision and accuracy of the algorithms and identifying any systematic 305 discrepancies (Chicco et al., 2021; Hodson, 2022). The complete set of equations used for the evaluation is included in Equations (S1)–(S6)

3 Results

3.1 Estimation of Kc based on vegetation index (VI) for ETa determination

The variations in Kc and NDVI across four cropping seasons are illustrated in Fig.4. During the 2019 cropping season 310 (Fig.4−a), the season began with relatively high Kc and NDVI values (0.86 and 0.8), suggesting that the crop was healthy and actively transpiring, with substantial green canopy cover. As the season advanced to around DOY 268, Kc and NDVI values gradually became closer (0.76 and 0.79), indicating consistent vegetation growth and stabilization of canopy greenness. Towards the end of the season (DOY 300), both indices declined to 0.43 and 0.38, reflecting the senescence phase of the crop marked by reduced greenness and water demand. In the 2019−2020 season (Fig.4−b), around DOY 316, both Kc and NDVI 315 values were low (0.41 and 0.37), representing the early growth stage with sparse vegetation and minimal transpiration. The indices reached their peak by DOY 31 in 2020, indicating the height of the crop's growth and greenness, before tapering off again to 0.4 and 0.35 as the season ended, consistent with the crop's natural lifecycle. On other Seasons as depicted on Fig. 4−c and Fig. 4−d: Similar trends were observed, wherein Kc and NDVI closely mirrored the crop development stages. During the early stages, the indices remained low, gradually increasing as the crop established its canopy. Peaks are the period of 320 maximum crop growth, followed by declines as the crop matured and approached senescence. A summary of Kc models derived through linear regression analysis between Kc and NDVI are shown in Table (S2), while the scatter plots between estimated ET and measured ETa are shown in Figure (S1).

https://doi.org/10.5194/hess-2024-351
Preprint. Discussion started: 3 February 2025

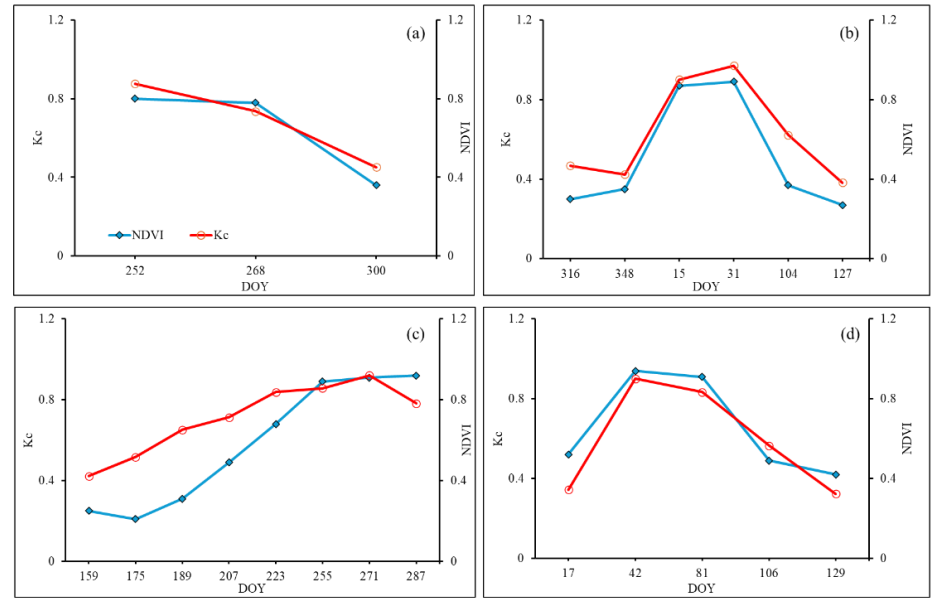

Figure 4. The variability of Kc values in relation to the changes in NDVI for the period 2019−2021 where (a) is the winter cropping season in 2019, (b) relates to 2019−2020 summer season, (c) is the 2020 winter season and (d) is the 2021 summer season calculated in the Southern Hemisphere.

3.2 The spatial distribution of ETa based on the four remote sensing algorithms

Figure 5 presents the spatial distribution of ETa variation across the irrigation scheme for the period between 9th September 2019 and 27th October 2019. The spatial distribution maps are at a 30-meter spatial resolution. The maps shown are based on four remote sensing algorithms used to estimate daily ETa on the satellite pass days when the Landsat 8 images were free of clouds. On all three dates, ETa estimates show variability due to changes in environmental conditions like temperature, radiation, and vegetation activity. ETa values tend to increase toward the later date (October 27), especially with SEBAL, VI-ETa and SEBS, reflecting seasonal dynamics or crop growth. High ETa values (red regions) concentrated in areas with dense vegetation or high soil moisture. Low ETa values (green regions) are in regions with less vegetation or water stress. SEBAL and SEBS consistently estimate higher ETa values compared to CWSI and VI. The differences between algorithms highlight the variability in their sensitivity to input parameters like vegetation indices, surface temperature and energy balance terms. These maps provided ETa evaluation pixels at different station locations within the irrigation scheme. The estimates of ETa by SEBS, SEBAL and VI-based were comparable in most cases, while the CWSI estimates were mostly lower or extremely high in certain cases. The VI-based ETa had a minimum of 0 mm d^{-1} which was a result of bare soil pixels which are uncaptured by vegetation indices when estimating ETa. The spatial distribution maps aided in providing correlation pixels for the

https://doi.org/10.5194/hess-2024-351
Preprint. Discussion started: 3 February 2025

Hydrology and Earth System Sciences
Discussions

evaluation. More maps which demonstrate the spatial distribution of ETa across the irrigation scheme are in Figures (S2) - (S6).

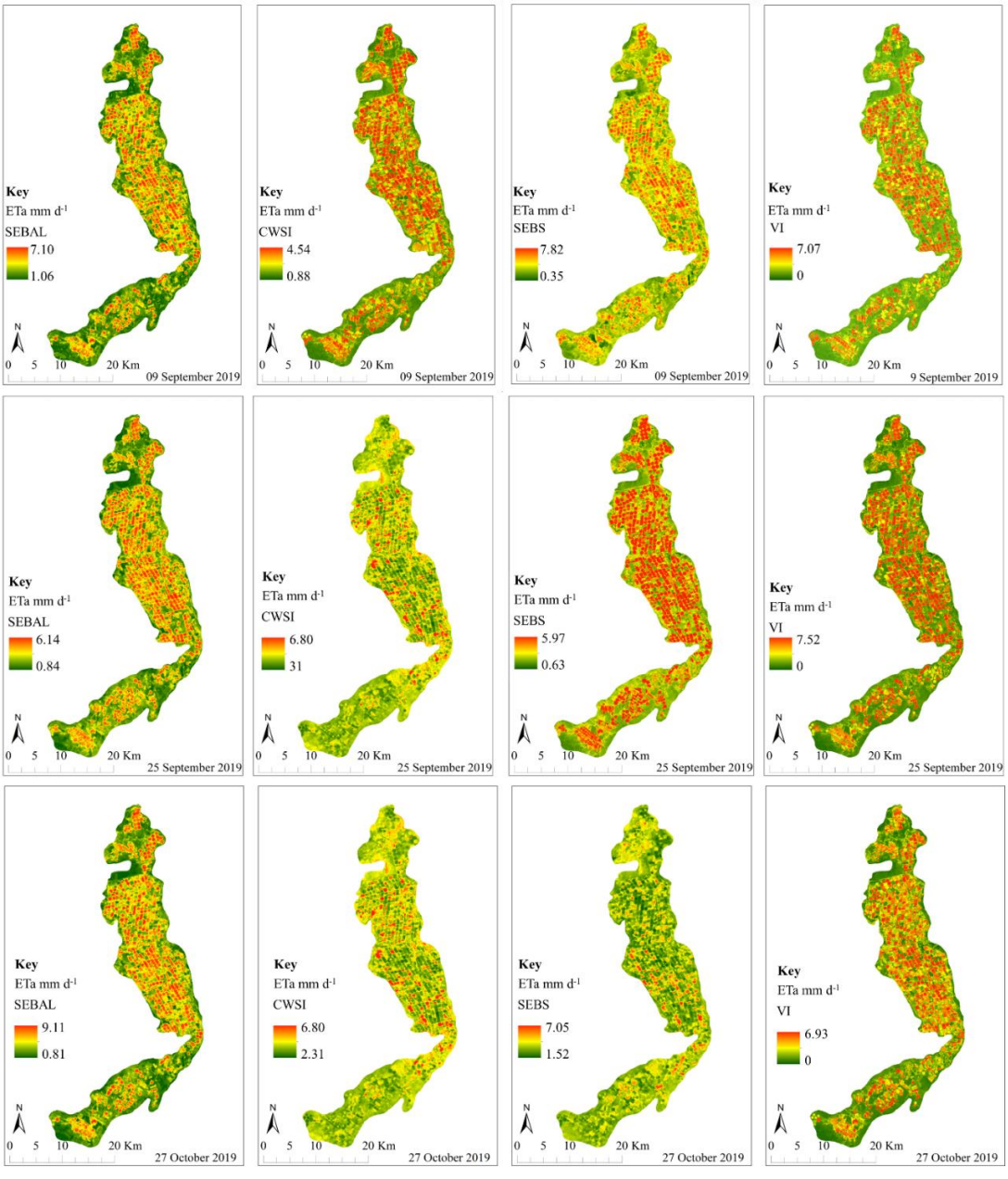

Figure 5. An example of the **spatial distribution of ETa within Vaalharts irrigation scheme estimated by SEBAL, CWSI, SEBS and VI-based algorithms for the 9th of September 2019 to 27th October 2019.**

https://doi.org/10.5194/hess-2024-351
Preprint. Discussion started: 3 February 2025

Hydrology and Earth System Sciences
Discussions

3.3 Evapotranspiration variability across different seasons and algorithms at the field scale

Figure 6 (a–d) presents the temporal trends between lysimeter ETa and ETa estimated using four algorithms at the field level. Figure 6–a shows the variations between lysimeter ETa and VI-ETa across the cropping seasons. The graphs indicate that, on most days, lysimeter ETa closely matched VI-ETa, with only slight underestimations and overestimations on some days. Overall, the differences were minimal. Figure 6–b compares lysimeter ETa with SEBAL algorithm estimates. Both methods exhibited similar trends, with SEBAL estimates increasing and decreasing in tandem with lysimeter ETa. Throughout the cropping seasons, both methods captured ETa fluxes similarly. However, SEBAL tended to overestimate ETa on most days, with evident overestimations on days of the year (DOY) 31, 130, 207, 287, and 113, and slight underestimations around DOY 320. Figure 6–c illustrates the relationship between lysimeter ETa and CWSI–ETa. Unlike the other algorithms, CWSI–ETa showed significant fluxes on most days, with values often surpassing those of lysimeter ETa. The lysimeter ETa displayed smoother variability compared to the more fluctuating CWSI–ETa values. Figure 6–d shows that SEBS ETa estimates closely tracked lysimeter ETa values, like the SEBAL and VI-ETa estimates. The scatter plots between the models and lysimeter ETa values is shown in Figure (S7).

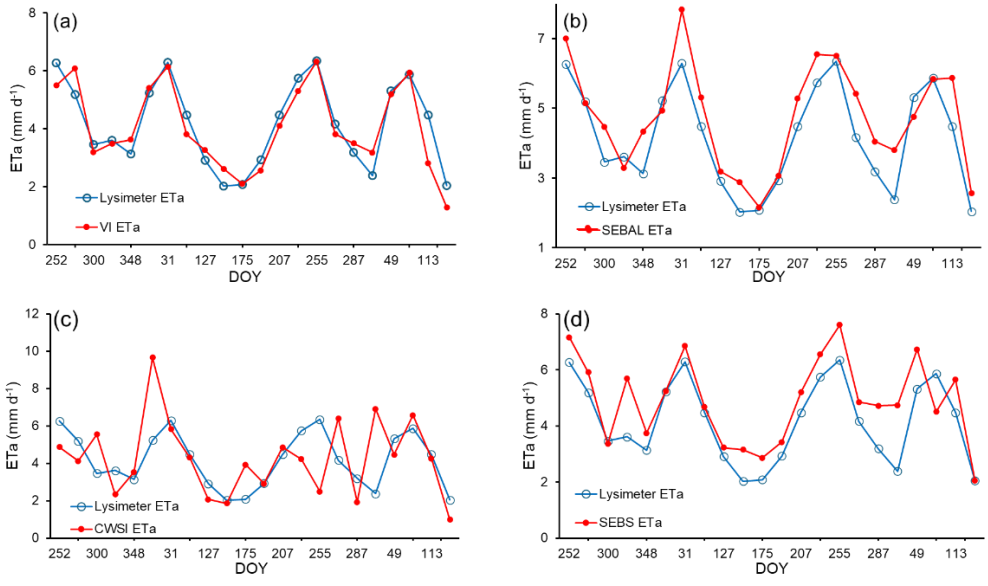

Figure 6. Variability of lysimeter ETa and estimated ETa by VI ETa (a), SEBAL (b), CWSI ETa (c) and SEBS (d) algorithms.

3.3.1 Summary of evaluation metrics for the four algorithms against the smart lysimeter at farm scale

The evaluation of SEBAL, VI, CWSI and SEBS ETa algorithms against the lysimeter measured ETa using statistical metrics shows significant differences in their performance as indicated on Fig.7. The SEBAL and VI algorithms demonstrate strong correlations with measured lysimeter ETa values where both have achieved high correlation coefficient (0.92) and R^2 values

https://doi.org/10.5194/hess-2024-351
Preprint. Discussion started: 3 February 2025

Hydrology and Earth System Sciences
Discussions

of 0.84 and 0.85, respectively which indicates a strong linear relationship. These methods exhibit the lowest RMSE and MAE values, indicating higher accuracy, with average prediction errors of 0.83 mm d^{-1} and 0.58 mm d^{-1} for RMSE, and 0.69 mm d^{-1} and 0.44 mm d^{-1} for MAE. The results are highly statistically significant, with p-values < 0.001. On the other hand, the CWSI-based ETa algorithm demonstrates a very low correlation coefficient of 0.42 with the R^2 value of 0.18, alongside higher RMSE of 1.91 mm d^{-1} and MAE of 1.40 mm d^{-1}, indicating poorer performance in both accuracy and explanation of variance. The SEBS algorithm demonstrated a strong correlation with the correlation coefficient of 0.86 and a substantial R^2 of 0.75 with higher errors on RMSE of 1.07 and MAE of 0.87, mm d^{-1} and greater variability in prediction errors with SE of 1.12 and a highly statistically significant correlations with p value <0.001. The bias values indicate that SEBAL and SEBS generally overestimate the measured values by 0.33 mm d^{-1} and 0.52 mm d^{-1}, respectively, whereas VI tends to slightly underestimate them, with an average bias of approximately -0.12 mm d^{-1}. However, the SEBAL and VI are the most reliable methods with lower error rates, whereas CWSI has the least effectiveness in accurately predicting the measured lysimeter ETa values with R^2 of 0.18, RMSE of 1.91, MAE of 1.40 and a p value <0.05 showing the result are not statistically significant.

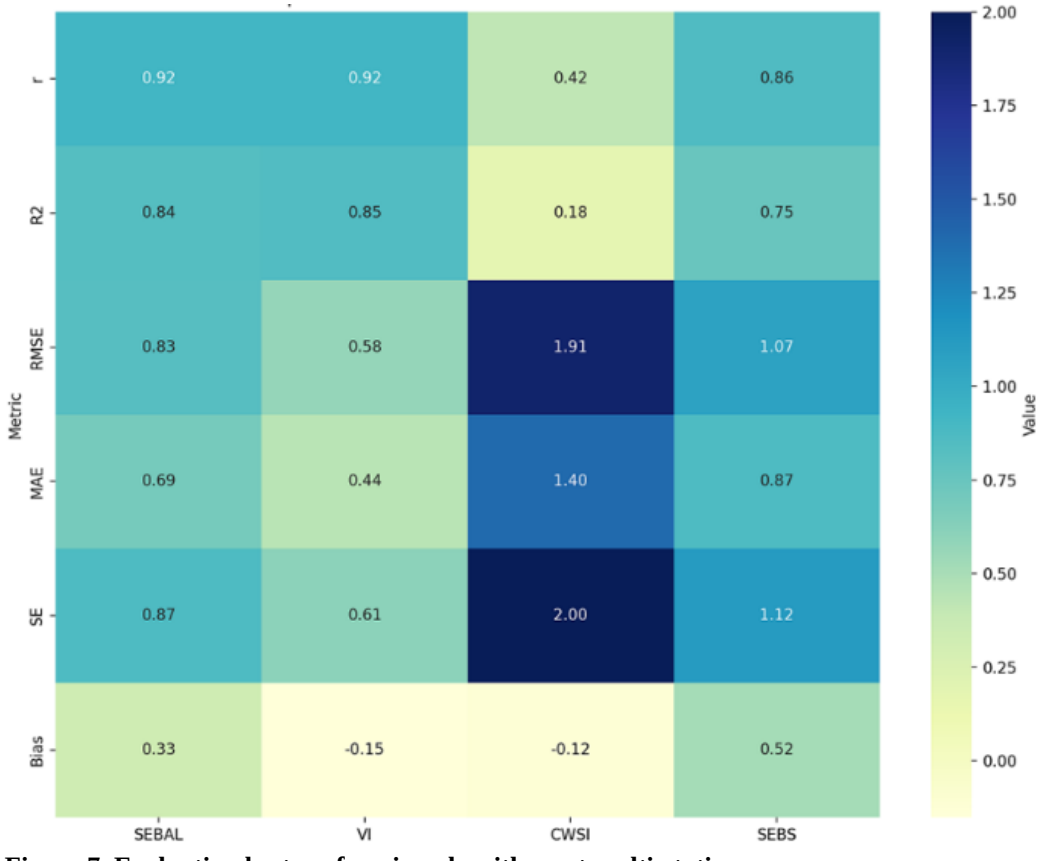

Figure 7. Evaluation best performing algorithms at multi-stations.

https://doi.org/10.5194/hess-2024-351
Preprint. Discussion started: 3 February 2025

Hydrology and Earth System Sciences
Discussions

3.4 Comparison of quantified ETa from all algorithms and measurements

Figure 8 shows a comparison of the total ETa estimates from 2019 to 2021 of cloud free Landsat 8 data across the four different algorithms: SEBAL, SEBS, VI-ETa, and CWSI-ETa against lysimeter-measured ETa in millimetres (mm). The total estimated ETa for each algorithm is represented by a bar in the corresponding colour. The lysimeter data acts as a benchmark of ETa, and differences in bar heights demonstrates how closely each algorithm aligns with the measured ETa. This reflection provides insight into the accuracy and reliability of the algorithms in estimating ETa over the study period. The total ETa measured by the lysimeter which matches the evaluated Landsat 8 images was 91.63 mm while SEBAL had a closer reading with only 1.41 mm. VI-based ETa followed with 2.36 mm which was followed by the SEBS algorithm with 5.63 mm difference whereas the CWSI-based ETa algorithm had the biggest difference of 16.24 mm over the evaluated period. These findings demonstrate the reliability of SEBAL, VI-based ETa and SEBS in accurately estimating ETa.

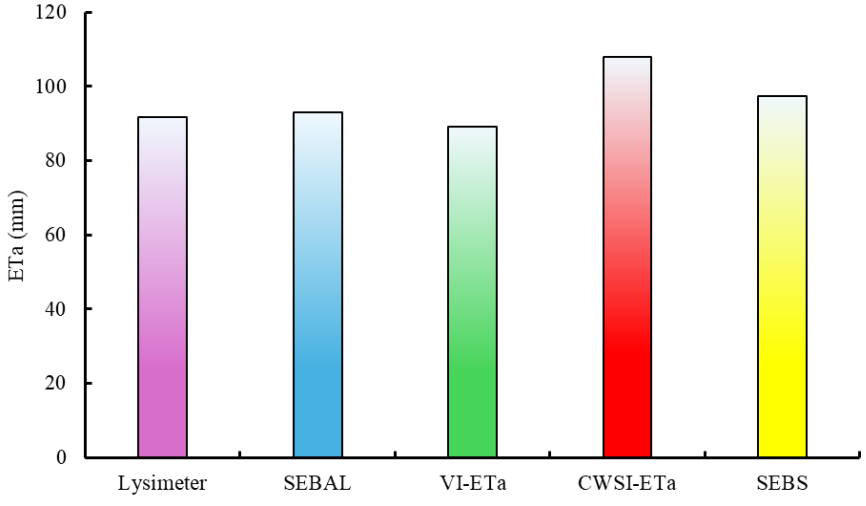

Figure 8. Total lysimeter measured and estimated ETa by SEBAL (blue), VI-ETa (green), CWSI (red) and SEBS (yellow) during the study period.

3.5 The statistical summary of evaluation of algorithms across pixels at different locations with weather stations

The findings for the three algorithms which demonstrated promising performance at field level: SEBAL, SEBS, and VI-based reveal distinct differences in their accuracy and reliability across the validation weather station locations (Table 2). The SEBAL algorithm consistently demonstrates robust performance, with high correlation values, indicating a close match between its ETa estimates and measured ETa data. The low error values reflect SEBAL's ability to make precise predictions with minimal bias, demonstrating its reliability across all sites. Although SEBS appears to be performing well, it shows more variability in its accuracy. Its correlation and determination coefficient values are slightly lower than SEBAL, while it exhibits higher prediction errors. This suggests that SEBS might be more sensitive to local environmental conditions or input data quality,

https://doi.org/10.5194/hess-2024-351
Preprint. Discussion started: 3 February 2025

Hydrology and Earth System Sciences Discussions

leading to moderate discrepancies in its ETa estimates compared to the measured ETa values. The VI-based ETa performs better than SEBS in certain cases but not as consistently as SEBAL. It shows moderate correlation and determination coefficient values, with errors slightly higher than SEBAL but lower than SEBS. The bias values suggest that VI-based ETa might overestimate or underestimate ETa depending on the site, yet its statistical significance remains strong.

Table 2. The statistical summary of performance of estimated daily ETa from SEBAL, VI, SEBS and CWSI based models with measured lysimeter ETa

Algorithm	**SEBAL ETa**				**SEBS ETa**				**VI ETa**			
Statistical Metric	SABBI	Tadcaster	Jankempdorp	Ganspan	SABBI	Tadcaster	Jankempdorp	Ganspan	SABBI	Tadcaster	Jankempdorp	Ganspan
r	0.93	0.94	0.96	0.91	0.89	0.81	0.90	0.78	0.90	0.80	0.90	0.86
R^2	0.87	0.88	0.92	0.83	0.80	0.66	0.81	0.61	0.82	0.63	0.80	0.73
RMSE	0.31	0.89	0.53	0.47	1.31	1.48	0.93	1.59	0.41	0.77	0.86	0.52
MAE	0.27	0.82	0.38	0.36	1.21	1.29	0.77	1.41	0.32	0.54	0.74	0.47
SE	0.10	0.31	0.19	0.17	0.17	0.52	0.33	0.56	0.12	0.27	0.31	0.19
Bias	0.01	0.70	0.26	-0.09	1.10	0.95	0.61	0.90	0.08	0.39	0.54	0.02
P value	<0.001	<0.001	<0.001	<0.001	<0.001	<0.001	<0.001	<0.001	<0.001	<0.001	<0.001	<0.001

3.6 The regression plot of algorithms ETa against the extrapolated ETa at different study area locations

Figure 9 demonstrates the scatter plots between ETa by each algorithm compared to extrapolated ETa on weather stations. The points displayed on each plot indicates the degree of correlation between the two sets of ETa values with those points along the line showing high correlations while those far apart indicates low correlations. The figure displays a series of scatter plots derived from the relationship between ETa estimated by each better performing algorithm and values of ETa extrapolated from lysimeter measurements with weather station measurements. The slope and alignment of the regression lines relative to the data points provide insight into the performance of each algorithm. The SEBAL approach shows regression lines closely aligned with the data, indicating strong agreement and a reliable estimation of ETa values, while the SEBS method displays greater variability, with data points more widely dispersed around the regression lines, reflecting less precise predictions compared to SEBAL. However, VI exhibits moderate performance, with data points closer to the regression lines than SEBS but not as tightly clustered as SEBAL.

https://doi.org/10.5194/hess-2024-351
Preprint. Discussion started: 3 February 2025

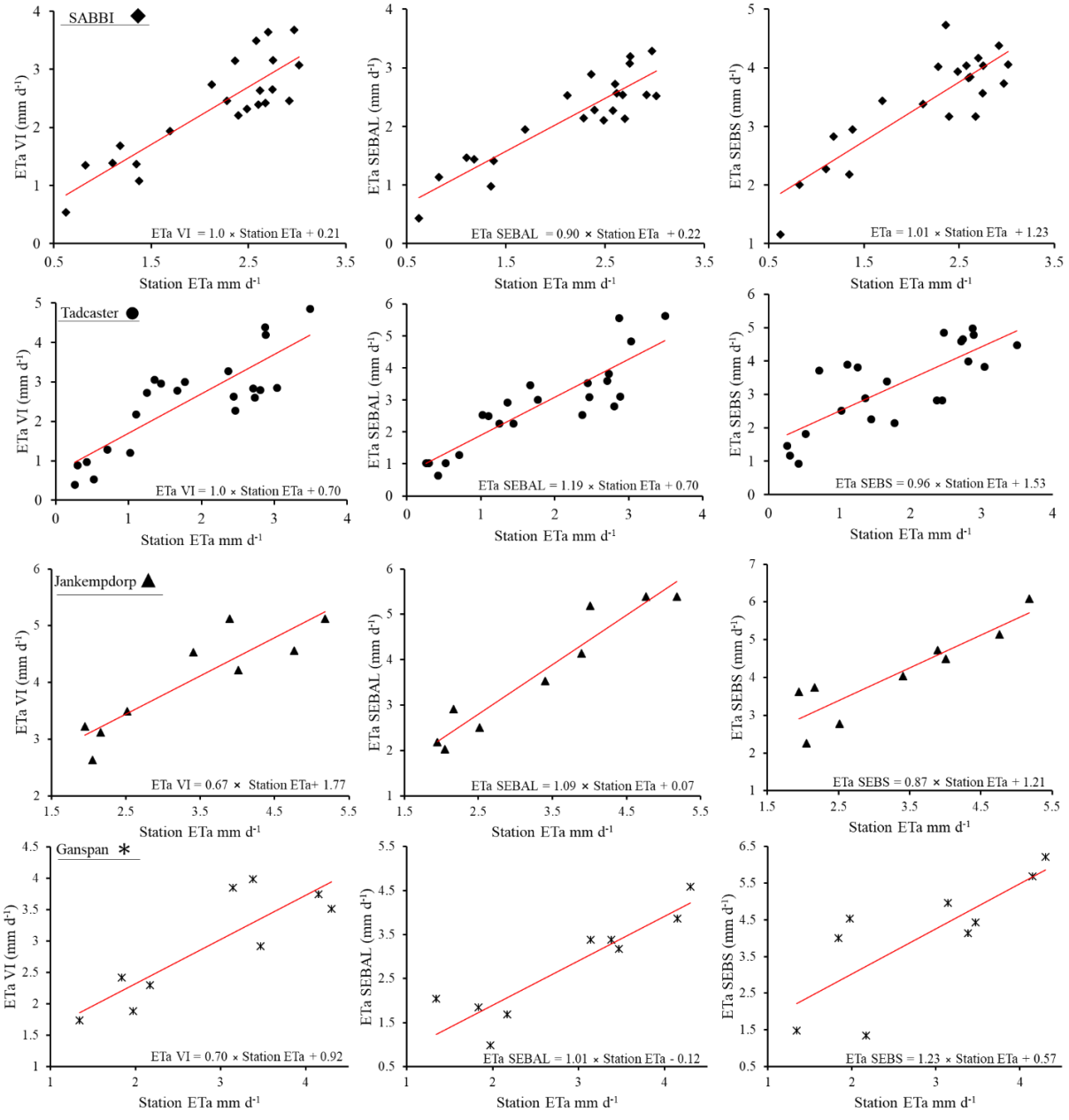

Figure 9. Scatter plots between ETa estimated using VI-ET, SEBAL and SEBS algorithms compared to extrapolated ETa on weather stations.

https://doi.org/10.5194/hess-2024-351
Preprint. Discussion started: 3 February 2025


Hydrology and Earth System Sciences Discussions

4 Discussion

In South Africa, water crisis significantly impacts livelihoods, this issue necessitates urgent measures to manage and equitably distribute water resources particularly in agriculture which is a major water user. To address this, remote sensing approaches using Landsat 8 images were used to estimate ETa using various algorithms (SEBAL, VI-ETa, CWSI-ETa and SEBS). Ground truth data from a smart field weighing lysimeter was used for calibrating and validating these estimates. Evaluations at both farm and scheme levels revealed that SEBAL was the most accurate algorithm, followed by VI-ETa and SEBS, while CWSI-ETa performed poorly.

The determination of ETa using the VI-ETa approach demonstrates the utility of NDVI as a reliable proxy for vegetation dynamics and crop water use. The strong linear relationship observed between NDVI and Kc shows NDVI's ability to capture phenological changes and crop development under unstressed conditions. These findings align with those of Niu et al. (2020), who reported a good correlation between NDVI and Kc values. This consistency across studies emphasizes the strength of NDVI-based methods in agricultural water management. The ensemble Kc model, developed through an integration of season-specific Kc models, exhibited exceptional accuracy in aligned with ground-derived Kc values. The model's capacity to generalize Kc across diverse vegetation types and cropping seasons shows its potential for broad applicability in irrigated schemes like the Vaalharts scheme which is characterized by diverse crops and horticultural practices.

Validation of VI-ETa approach in estimating ETa against lysimeter measurements demonstrated its reliability with strong correlations and low error metrics. The slight underestimation of ETa, which reflected in a negative bias, suggests potential for fine-tuning the algorithm to account for localized environmental or crop-specific conditions. These results reflect the findings by Jarchow et al. (2022), who reported comparable accuracy in lysimeter-based validations. However, the VI-ETa approach also has limitations which were observed. For instance, the algorithm's dependence on vegetation surfaces restricts its utility in quantifying bare soil evaporation, necessitating complementary methods to address evaporation in sparsely vegetated areas. This limitation signifies an area for future refinement particularly in mixed land-use systems or early-season conditions with minimal vegetation cover. Beyond field-scale validations, the extrapolation of ETa estimates to broader spatial scales demonstrates the practicality of the algorithm for regional water resource management. The ability to estimate Kc values over large areas enhances precision irrigation planning and monitoring, this demonstrates critical needs in agricultural water management. The VI-ETa algorithm's performance in this study was enhanced by the ensemble Kc model which captures the diversity in vegetation phenology and water requirement which offers a reliable and scalable method for estimating crop water use.

The SEBAL algorithm demonstrated a strong performance in estimating ETa, as evidenced by its statistical indicators. However, a slight positive bias indicates a tendency for overestimation. In instances where estimates from SEBAL are used

https://doi.org/10.5194/hess-2024-351
Preprint. Discussion started: 3 February 2025


Hydrology and Earth System Sciences Discussions

for crop water requirements, the overestimation can be accounted for during irrigation scheduling to reduce the overuse of water. Despite the obtained minor overestimations on this study, SEBAL algorithm remains one of the most reliable algorithms for ETa estimation which provides a good balance between complexity and accuracy (Allen et al., 1998). The performance aligns with some previous studies which applied SEBAL algorithm, for instance, Shoko et al. (2015) demonstrated SEBAL's efficacy in a South African context, where it achieved high accuracy using Landsat 8 and MODIS data validated against eddy covariance system measurements. They reported lower values being estimated using MODIS data with ETa difference compared to Landsat 8 estimates. Allen et al. (1998) validated SEBAL's estimates against lysimeter ETa measurements, confirming its suitability for watershed-scale applications. Although these comparisons affirm the reliability of SEBAL, they also highlight its adaptability across various environmental and spatial scales. The slight overestimation observed in this study may stem from assumptions inherent in SEBAL's parameterization such as surface albedo and aerodynamic resistance, which could vary under specific microclimatic conditions. Moreover, the resolution of the input satellite data plays a role; higher-resolution datasets, like those from Landsat 8, tend to improve estimation accuracy although it may still introduce minor discrepancies depending on land cover heterogeneity.

On the other hand, the CWSI-based ETa estimation showed the weakest performance among all algorithms evaluated, with weak statistical metrics. These findings suggest that CWSI-based method may not be suitable for precise ETa estimation in environments characterized by high variability in land use and water stress regimes. The poor performance of CWSI algorithm can be attributed to the method's reliance on capturing thermal dynamics which poses challenges, this is typically the case when using thermal data with coarse resolution such as the 90 m spatial resolution of Landsat 8 satellite. Katimbo et al. (2022) highlighted the sensitivity of CWSI to soil water depletion, particularly when levels drop below 80% of field capacity. This sensitivity becomes problematic in arid environments where moisture deficits are pronounced and soil moisture fluctuates significantly, leading to inaccuracies in ETa estimation. Furthermore, studies by Liu et al. (2022) and Boyaci et al. (2024) have demonstrated that the performance of CWSI is influenced by factors including crop type, environmental conditions, and calibration of temperature measurements. These factors contribute to variability in how well CWSI reflects ETa rates. In this study, such variability may have limited the method's effectiveness in capturing the dynamic water stress conditions experienced by crops. While the CWSI provides a temperature-based indication of water stress, it does not fully account for other critical factors influencing ET, such as atmospheric evaporative demand and plant physiological responses. This limitation, as discussed by Liu et al. (2022), may explain the observed discrepancies and demonstrates the need for caution when applying CWSI in areas where environmental and crop conditions vary significantly.

The SEBS algorithm showed a strong potential in estimating ETa at the field level when compared against smart field weighing lysimeter measurements. However, its performance varied across different validation sites, with the lowest correlation observed at Ganspan validation site. Despite this variability, the results suggest that SEBS estimates generally maintain a strong linear relationship with ground-based measurements and extrapolated ETa values, confirming the algorithm's reliability

https://doi.org/10.5194/hess-2024-351
Preprint. Discussion started: 3 February 2025

under specific conditions. Nevertheless, certain limitations of SEBS were evident. The algorithm exhibited higher errors compared to SEBAL with a tendency to overestimate ETa. This overestimation may reflect the algorithm's sensitivity to input parameters or specific environmental conditions, suggesting the need for calibration to improve its accuracy in heterogeneous settings such as the Vaalharts irrigation scheme. Similar observations have been reported in other studies. For example, McCabe and Wood (2006) and Dobriyal et al. (2012) noted overestimations in forested areas, while Rwasoka et al. (2011) observed daily overestimations in grasslands. The heterogeneous environment which comprised of pecan trees, natural vegetation, grass and diverse crops likely contributed to the observed overestimation. The shared thermal pixels between different land covers may have skewed heat flux estimates when different land covers exist in one pixel. Moreover, findings from South Africa's Gibson et al. (2011) and Gokool et al. (2018) affirms the influence of climatic conditions and validation methodologies on SEBS performance. Gibson et al. (2011) observed overestimations under wet conditions, while Gokool's study in a sub-humid sugarcane farm reported low accuracies associated with ground measurement uncertainties. These findings highlight the importance of using accurate devices like weighing lysimeters and higher-resolution Landsat data, as done in this study, to improve SEBS calibration and applicability.

The evaluation of these algorithms highlights their respective strengths and limitations in estimating ETa within a heterogeneous irrigation scheme. SEBAL, VI-ETa and SEBS demonstrated strong potential for water management applications, while CWSI-ETa requires further refinement to address its limitations. The role of input data spatial resolution and the challenges of extrapolating ETa through weather stations from lysimeter measurements are critical considerations for enhancing the accuracy and applicability of these models. Weather stations and lysimeters provide point-based measurements, which might not capture the spatial dynamics across larger areas. This mismatch can result in over- or underestimation when scaling up. Errors in weather station data such as: temperature, wind speed and humidity measurements can propagate when used to validate or calibrate ETa models for larger areas. Moreover, algorithms may struggle to accurately account for varying levels of water stress across regions, particularly in arid zones where rapid moisture changes occur.

5 Conclusions

In this study four algorithms: SEBAL, SEBS, VI-ETa and CWSI-ETa were used to estimate ETa which was evaluated using a smart field weighing lysimeter measured ETa. The findings demonstrated that among the evaluated, SEBAL and VI-ETa demonstrated the best performance, with strong accuracy and reliability. SEBAL showed high accuracy at both farm and scheme scales, making it a valuable tool for ETa estimation and water management. Although the study was conducted within the Vaalharts irrigation scheme, algorithms like SEBAL and VI-ETa demonstrate strong potential for widespread application in regions with comparable cropping systems and water resource challenges. For instance, the strong correlation between NDVI and Kc demonstrates the universal applicability of NDVI-based approaches for monitoring crop water use in diverse agricultural settings. However, the distinctiveness of the results also highlights critical site-specific complexities. The observed

https://doi.org/10.5194/hess-2024-351
Preprint. Discussion started: 3 February 2025


Hydrology and Earth System Sciences Discussions

algorithm performances, particularly the limitations of CWSI-ETa in arid zones, point to the necessity of adapting models to local climatic and environmental conditions. Variations in microclimate, crop type and irrigation practices across regions can influence the reliability and accuracy of ETa estimates. The findings of this study make emphasis on the importance of integrating high-resolution satellite data with ground-based measurements to improve ETa estimation accuracy. Although the findings align with global literature, regional or site-specific local validations remain essential to account for localized factors such as soil heterogeneity and mixed land-use systems. This is key considering the limitations of direct ETa measurements in most parts of South Africa. The focus on general principles and site-specific adaptations can provide a framework for scaling these approaches to other regions. The revisit period of Landsat 8 also stands out as a key challenge in using ETa estimates for continuous irrigation scheduling particularly for crops that require frequent irrigation.

6 Suggestions for further research

Future studies should prioritise improving the CWSI-based algorithm by using higher-resolution thermal datasets and better calibration methods to improve accuracy in environments with diverse land use and water stress regimes. Complementary techniques, such as combining VI-based models with additional indices, are critical for overcoming constraints in estimating bare soil evaporation, particularly in sparsely vegetated or early-season settings. Comprehensive field validations across diverse land use types and climates in South Africa are critical for increasing ETa model resilience. Given the lack of ETa data in Africa, it is critical to deploy advanced measuring tools such as eddy covariance systems and high-precision lysimeters with open-access policies to ensure a wide-scale evaluations of ETa algorithms. Future studies should also modify and test algorithms in various geographic regions and agricultural systems to ensure their broader application.

7 Statements and Declarations

Funding: This study was funded by the Water Research Commission (WRC) of South Africa under the project: C2022_2023−00978 and the Agricultural Research Council (ARC) of South Africa under the crop estimate project: ISC01203000027.

Competing interests: Authors declare no personal or financial interests that has any influence on the quality of this work.

Author contributions: PER: conceptualization, data curation, formal analysis, investigation, methodology, software, validation, visualization, and writing – original draft preparation. MAM, EA, GC: conceptualization, funding acquisition, investigation, project administration, supervision, validation, and writing – original draft preparation.

Data availability: Data used and generated for this study are included in the article through links while some data is available on request.

https://doi.org/10.5194/hess-2024-351
Preprint. Discussion started: 3 February 2025

Hydrology and Earth System Sciences
Discussions

References

Abbasi, N., Nouri, H., Didan, K., Barreto-Muñoz, A., Chavoshi Borujeni, S., Salemi, H., Opp, C., Siebert, S., and Nagler, P.: Estimating Actual Evapotranspiration over Croplands Using Vegetation Index Methods and Dynamic Harvested Area, Remote Sens., 13, 5167, https://doi.org/10.3390/rs13245167, 2021.

Allen, R. G., Pereira, L. S., Raes, D., and Smith, M.: Crop Evapotranspiration-Guidelines for computing crop water requirements-FAO Irrigation and drainage paper 56, Fao Rome, 300, D05109, 1998.

Allen, R. G., Tasumi, M., and Trezza, R.: Satellite-Based Energy Balance for Mapping Evapotranspiration with Internalized Calibration (METRIC)—Model, J. Irrig. Drain. Eng., 133, 380–394, https://doi.org/10.1061/(ASCE)0733-9437(2007)133:4(380), 2007.

Bastiaanssen, W. G. M.: SEBAL-based sensible and latent heat fluxes in the irrigated Gediz Basin, Turkey, J. Hydrol., 229, 87–100, 2000.

Bastiaanssen, W. G. M., Noordman, E. J. M., Pelgrum, H., Davids, G., Thoreson, B. P., and Allen, R. G.: SEBAL Model with Remotely Sensed Data to Improve Water-Resources Management under Actual Field Conditions, J. Irrig. Drain. Eng., 131, 85–93, https://doi.org/10.1061/(ASCE)0733-9437(2005)131:1(85), 2005.

Blatchford, M. L., Mannaerts, C. M., Njuki, S. M., Nouri, H., Zeng, Y., Pelgrum, H., Wonink, S., and Karimi, P.: Evaluation of WAPOR V2 evapotranspiration products across Africa, Hydrol. Process., 34, 3200–3221, https://doi.org/10.1002/hyp.13791, 2020.

Boyaci, S., Kocięcka, J., Atilgan, A., Liberacki, D., Rolbiecki, R., Saltuk, B., and Stachowski, P.: Evaluation of Crop Water Stress Index (CWSI) for High Tunnel Greenhouse Tomatoes under Different Irrigation Levels, Atmosphere, 15, 205, https://doi.org/10.3390/atmos15020205, 2024.

Chicco, D., Warrens, M. J., and Jurman, G.: The coefficient of determination R-squared is more informative than SMAPE, MAE, MAPE, MSE and RMSE in regression analysis evaluation, PeerJ Comput. Sci., 7, e623, https://doi.org/10.7717/peerj-cs.623, 2021.

Dalton, J.: Experimental essays, on the constitution of mixed gases; on the force of steam or vapour from water and other liquids in different temperatures, both in a Torricellian vacuum and in air; on evaporation; and on the expansion of elastic fluids by heat, No Title, 1802.

Djaman, K., Rudnick, D. R., Moukoumbi, Y. D., Sow, A., and Irmak, S.: Actual evapotranspiration and crop coefficients of irrigated lowland rice (Oryza sativa L.) under semiarid climate, 2019.

Djaman, K., Mohammed, A. T., and Koudahe, K.: Accuracy of Estimated Crop Evapotranspiration Using Locally Developed Crop Coefficients against Satellite-Derived Crop Evapotranspiration in a Semiarid Climate, Agronomy, 13, 1937, https://doi.org/10.3390/agronomy13071937, 2023.

Dobriyal, P., Qureshi, A., Badola, R., and Hussain, S. A.: A review of the methods available for estimating soil moisture and its implications for water resource management, J. Hydrol., 458–459, 110–117, https://doi.org/10.1016/j.jhydrol.2012.06.021, 2012.

Doležal, F., Hernandez-Gomis, R., Matula, S., Gulamov, M., Miháliková, M., and Khodjaev, S.: Actual Evapotranspiration of Unirrigated Grass in a Smart Field Lysimeter, Vadose Zone J., 17, 1–13, https://doi.org/10.2136/vzj2017.09.0173, 2018.

https://doi.org/10.5194/hess-2024-351
Preprint. Discussion started: 3 February 2025

Elfarkh, J., Simonneaux, V., Jarlan, L., Ezzahar, J., Boulet, G., Chakir, A., and Er-Raki, S.: Evapotranspiration estimates in a traditional irrigated area in semi-arid Mediterranean. Comparison of four remote sensing-based models, Agric. Water Manag., 270, 107728, https://doi.org/10.1016/j.agwat.2022.107728, 2022.

Gibson, L., Munch, Z., Carstens, M., and Conrad, J.: Remote sensing evapotranspiration (SEBS) evaluation using water balance, Water Research Commission, 2011.

Gibson, L., Jarmain, C., Su, Z., and Eckardt, F.: Review: Estimating evapotranspiration using remote sensing and the Surface Energy Balance System – A South African perspective, Water SA, 39, https://doi.org/10.4314/wsa.v39i4.5, 2013.

Glenn, E. P., Nagler, P. L., and Huete, A. R.: Vegetation Index Methods for Estimating Evapotranspiration by Remote Sensing, Surv. Geophys., 31, 531–555, https://doi.org/10.1007/s10712-010-9102-2, 2010.

Gokool, S., Riddell, E. S., Swemmer, A., Nippert, J. B., Raubenheimer, R., and Chetty, K. T.: Estimating groundwater contribution to transpiration using satellite-derived evapotranspiration estimates coupled with stable isotope analysis, J. Arid Environ., 152, 45–54, 2018.

Hodson, T. O.: Root-mean-square error (RMSE) or mean absolute error (MAE): when to use them or not, Geosci. Model Dev., 15, 5481–5487, https://doi.org/10.5194/gmd-15-5481-2022, 2022.

Hunsaker, D. J., Pinter, P. J., and Kimball, B. A.: Wheat basal crop coefficients determined by normalized difference vegetation index, Irrig. Sci., 24, 1–14, https://doi.org/10.1007/s00271-005-0001-0, 2005.

Ingrao, C., Strippoli, R., Lagioia, G., and Huisingh, D.: Water scarcity in agriculture: An overview of causes, impacts and approaches for reducing the risks, Heliyon, 9, e18507, https://doi.org/10.1016/j.heliyon.2023.e18507, 2023.

Jackson, R. D., Idso, S. B., Reginato, R. J., and Pinter, P. J.: Canopy temperature as a crop water stress indicator, Water Resour. Res., 17, 1133–1138, https://doi.org/10.1029/WR017i004p01133, 1981.

Jarchow, C. J., Waugh, W. J., and Nagler, P. L.: Calibration of an evapotranspiration algorithm in a semiarid sagebrush steppe using a 3-ha lysimeter and Landsat normalized difference vegetation index data, Ecohydrology, 15, e2413, https://doi.org/10.1002/eco.2413, 2022.

Jiang, L., Wu, H., Tao, J., Kimball, J. S., Alfieri, L., and Chen, X.: Satellite-Based Evapotranspiration in Hydrological Model Calibration, Remote Sens., 12, 428, https://doi.org/10.3390/rs12030428, 2020.

Katimbo, A., Rudnick, D. R., DeJonge, K. C., Lo, T. H., Qiao, X., Franz, T. E., Nakabuye, H. N., and Duan, J.: Crop water stress index computation approaches and their sensitivity to soil water dynamics, Agric. Water Manag., 266, 107575, https://doi.org/10.1016/j.agwat.2022.107575, 2022.

Li, X., Yang, Y., Zhou, X., Han, S., Li, H., Yang, Y., and Hao, X.: Accuracy evaluation of ET and its components from three remote sensing ET models and one process based hydrological model using ground measured eddy covariance and sap flow, J. Hydrol., 626, 130374, https://doi.org/10.1016/j.jhydrol.2023.130374, 2023.

Lian, T., Xin, X., Peng, Z., Li, F., Zhang, H., Yu, S., and Liu, H.: Estimating Evapotranspiration over Heterogeneous Surface with Sentinel-2 and Sentinel-3 Data: A Case Study in Heihe River Basin, Remote Sens., 14, 1349, https://doi.org/10.3390/rs14061349, 2022.

https://doi.org/10.5194/hess-2024-351
Preprint. Discussion started: 3 February 2025

Liu, L., Gao, X., Ren, C., Cheng, X., Zhou, Y., Huang, H., Zhang, J., and Ba, Y.: Applicability of the crop water stress index based on canopy–air temperature differences for monitoring water status in a cork oak plantation, northern China, Agric. For. Meteorol., 327, 109226, https://doi.org/10.1016/j.agrformet.2022.109226, 2022.

Maisela, R. J.: Realizing agricultural potential in land reform: The case of Vaalharts irrigation scheme in the Northern Cape Province, Thesis, University of the Western Cape, 2007.

McCabe, M. F. and Wood, E. F.: Scale influences on the remote estimation of evapotranspiration using multiple satellite sensors, Remote Sens. Environ., 105, 271–285, https://doi.org/10.1016/j.rse.2006.07.006, 2006.

Mckenzie, R. L., Paulin, K. J., Bodeker, G. E., Liley, J. B., and Sturman, A. P.: Cloud cover measured by satellite and from the ground: Relationship to UV radiation at the surface, Int. J. Remote Sens., 19, 2969–2985, https://doi.org/10.1080/014311698214370, 1998.

McNamara, I., Baez-Villanueva, O. M., Zomorodian, A., Ayyad, S., Zambrano-Bigiarini, M., Zaroug, M., Mersha, A., Nauditt, A., Mbuliro, M., Wamala, S., and Ribbe, L.: How well do gridded precipitation and actual evapotranspiration products represent the key water balance components in the Nile Basin? J. Hydrol. Reg. Stud., 37, 100884, https://doi.org/10.1016/j.ejrh.2021.100884, 2021.

Meijninger, W. and Jarmain, C.: Satellite-based annual evaporation estimates of invasive alien plant species and native vegetation in South Africa, Water SA, 40, 95, https://doi.org/10.4314/wsa.v40i1.12, 2014.

Meyer, A.: Concerning several relationships between climate and soil in Europe, Chem. Erde, 2, 209–347, 1926.

Moeletsi, M. E., Myeni, L., Kaempffer, L. C., Vermaak, D., de Nysschen, G., Henningse, C., Nel, I., and Rowswell, D.: Climate Dataset for South Africa by the Agricultural Research Council, Data, 7, 117, 2022.

Mu, Q., Zhao, M., and Running, S. W.: Improvements to a MODIS global terrestrial evapotranspiration algorithm, Remote Sens. Environ., 115, 1781–1800, 2011.

Mukiibi, A., Franke, A. C., and Steyn, J. M.: Determination of Crop Coefficients and Evapotranspiration of Potato in a Semi-Arid Climate Using Canopy State Variables and Satellite-Based NDVI, Remote Sens., 15, 4579, https://doi.org/10.3390/rs15184579, 2023.

Mulovhedzi, N. E., Araya, N. A., Mengistu, M. G., Fessehazion, M. K., Du Plooy, C. P., Araya, H. T., and Van der Laan, M.: Estimating evapotranspiration and determining crop coefficients of irrigated sweet potato (Ipomoea batatas) grown in a semi-arid climate, Agric. Water Manag., 233, 106099, 2020.

Nagler, P., Glenn, E., Nguyen, U., Scott, R., and Doody, T.: Estimating Riparian and Agricultural Actual Evapotranspiration by Reference Evapotranspiration and MODIS Enhanced Vegetation Index, Remote Sens., 5, 3849–3871, https://doi.org/10.3390/rs5083849, 2013.

Ncoyini, Z., Savage, M. J., and Strydom, S.: Limited access and use of climate information by small-scale sugarcane farmers in South Africa: A case study, Clim. Serv., 26, 100285, https://doi.org/10.1016/j.cliser.2022.100285, 2022.

Ndou, N. N., Palamuleni, L. G., and Ramoelo, A.: Modelling depth to groundwater level using SEBAL-based dry season potential evapotranspiration in the upper Molopo River Catchment, South Africa, Egypt. J. Remote Sens. Space Sci., 21, 237–248, https://doi.org/10.1016/j.ejrs.2017.08.003, 2018.

https://doi.org/10.5194/hess-2024-351
Preprint. Discussion started: 3 February 2025

Niu, H., Hollenbeck, D., Zhao, T., Wang, D., and Chen, Y.: Evapotranspiration Estimation with Small UAVs in Precision Agriculture, Sensors, 20, 6427, https://doi.org/10.3390/s20226427, 2020.

Ojo, O. I.: Mapping and modeling of irrigation induced salinity of Vaalharts irrigation scheme in South Africa, PhD Thesis, Tshwane University of Technology, 2013.

Ojo, O. I., Ochieng, G. M., and Otieno, F. O. A.: Assessment of water logging and salinity problems in South Africa: an overview of Vaal Harts irrigation scheme, Water Soc., 153, 477–484, 2011.

Pandey, P. K., Dabral, P. P., and Pandey, V.: Evaluation of reference evapotranspiration methods for the northeastern region of India, Int. Soil Water Conserv. Res., 4, 52–63, https://doi.org/10.1016/j.iswcr.2016.02.003, 2016.

Peters, A., Nehls, T., Schonsky, H., and Wessolek, G.: Separating precipitation and evapotranspiration from noise–a new filter routine for high-resolution lysimeter data, Hydrol. Earth Syst. Sci., 18, 1189–1198, 2014.

Pretorius, W. M.: Vaalharts: environmental aspects of agricultural land and water use practices, PhD Thesis, North-West University, 2018.

Ramoelo, A., Majozi, N., Mathieu, R., Jovanovic, N., Nickless, A., and Dzikiti, S.: Validation of Global Evapotranspiration Product (MOD16) using Flux Tower Data in the African Savanna, South Africa, Remote Sens., 6, 7406–7423, https://doi.org/10.3390/rs6087406, 2014.

Ratshiedana, P. E.: Monitoring crop water use using unmanned aerial vehicle (UAV) and surface energy balance algorithms: a case study of Vaalharts Irrigation Scheme, Northern Cape Province, South Africa, 2022.

Raza, A., Al-Ansari, N., Hu, Y., Acharki, S., Vishwakarma, D. K., Aghelpour, P., Zubair, M., Wandolo, C. A., and Elbeltagi, A.: Misconceptions of Reference and Potential Evapotranspiration: A PRISMA-Guided Comprehensive Review, Hydrology, 9, 153, https://doi.org/10.3390/hydrology9090153, 2022.

Rosa, L., Chiarelli, D. D., Rulli, M. C., Dell'Angelo, J., and D'Odorico, P.: Global agricultural economic water scarcity, Sci. Adv., 6, eaaz6031, https://doi.org/10.1126/sciadv.aaz6031, 2020.

Rwasoka, D. T., Gumindoga, W., and Gwenzi, J.: Estimation of actual evapotranspiration using the Surface Energy Balance System (SEBS) algorithm in the Upper Manyame catchment in Zimbabwe, Phys. Chem. Earth Parts ABC, 36, 736–746, https://doi.org/10.1016/j.pce.2011.07.035, 2011.

Saha, S. K., Ahmmed, R., and Jahan, N.: Actual Evapotranspiration Estimation Using Remote Sensing: Comparison of Sebal and Metric Models, in: Water Management: A View from Multidisciplinary Perspectives, edited by: Tarekul Islam, G. M., Shampa, S., and Chowdhury, A. I. A., Springer International Publishing, Cham, 365–383, https://doi.org/10.1007/978-3-030-95722-3_18, 2022.

Sharma, B., Molden, D., and Cook, S.: Water use efficiency in agriculture: Measurement, current situation and trends, 2015.

Shoko, C., Clark, D., Mengistu, M., Dube, T., and Bulcock, H.: Effect of spatial resolution on remote sensing estimation of total evaporation in the uMngeni catchment, South Africa, J. Appl. Remote Sens., 9, 095997, https://doi.org/10.1117/1.JRS.9.095997, 2015.

Singels, A., Jarmain, C., Bastidas-Obando, E., Olivier, F., and Paraskevopoulos, A.: Monitoring water use efficiency of irrigated sugarcane production in Mpumalanga, South Africa, using SEBAL, Water SA, 44, https://doi.org/10.4314/wsa.v44i4.12, 2018.

https://doi.org/10.5194/hess-2024-351
Preprint. Discussion started: 3 February 2025


Hydrology and Earth System Sciences
Discussions

Su, Z.: The Surface Energy Balance System (SEBS) for estimation of turbulent heat fluxes, Hydrol. Earth Syst. Sci., 6, 85–100, https://doi.org/10.5194/hess-6-85-2002, 2002.

Tan, L., Zheng, K., Zhao, Q., and Wu, Y.: Evapotranspiration Estimation Using Remote Sensing Technology Based on a SEBAL Model in the Upper Reaches of the Huaihe River Basin, Atmosphere, 12, 1599, https://doi.org/10.3390/atmos12121599, 2021.

Tran, B. N., Van Der Kwast, J., Seyoum, S., Uijlenhoet, R., Jewitt, G., and Mul, M.: Uncertainty assessment of satellite remote-sensing-based evapotranspiration estimates: a systematic review of methods and gaps, Hydrol. Earth Syst. Sci., 27, 4505–4528, https://doi.org/10.5194/hess-27-4505-2023, 2023.

USGS: https://earthexplorer.usgs.gov/, 2022. Accessed: 04 February 2023

Verwey, P. and Vermeulen, P.: Influence of irrigation on the level, salinity and flow of groundwater at Vaalharts Irrigation Scheme, Water SA, 37, https://doi.org/10.4314/wsa.v37i2.65861, 2011.

Wang, Y., Hu, J., Li, R., Song, B., Hailemariam, M., Fu, Y., and Duan, J.: Increasing Cloud Coverage Deteriorates Evapotranspiration Estimating Accuracy from Satellite, Reanalysis and Land Surface Models Over East Asia, Geophys. Res. Lett., 50, e2022GL102706, https://doi.org/10.1029/2022GL102706, 2023.

Yan, C.: The Three-Temperature Model to Estimate Evapotranspiration and its Partitioning at Multiple Scales: A Review, Trans. ASABE, 59, 661–670, https://doi.org/10.13031/trans.59.11087, 2016.

Zamani Losgedaragh, S. and Rahimzadegan, M.: Evaluation of SEBS, SEBAL, and METRIC models in estimation of the evaporation from the freshwater lakes (Case study: Amirkabir dam, Iran), J. Hydrol., 561, 523–531, https://doi.org/10.1016/j.jhydrol.2018.04.025, 2018.